Hydrodynamic magnetoresistance in graphene Corbino devices

Alex Levchenko¹, Songci Li¹, and A. V. Andreev²

Department of Physics, University of Wisconsin-Madison, Madison, Wisconsin 53706, USA

Department of Physics, University of Washington, Seattle, Washington 98195, USA



(Received 1 September 2022; accepted 16 November 2022; published 28 November 2022)

We study hydrodynamic electron magnetotransport in graphene devices. We show that in these systems a distinct mechanism of magnetoresistance appears which is absent in systems with Galilean-invariant electron liquid. The resulting magnetoresistance depends on the intrinsic conductivity and viscosity of the electron liquid, and becomes especially pronounced near charge neutrality. We obtain analytic expressions for magnetotransport coefficients of Corbino devices and obtain estimates for the electrical and thermal magnetoresistances for monolayer and bilayer systems at charge neutrality. Magnetoresistance becomes strong (of order 100%) at relatively weak fields, at which the kinetic coefficients of the electron liquid are practically unaffected by the magnetic field.

DOI: 10.1103/PhysRevB.106.L201306

I. INTRODUCTION

Much of the recent interest in the electronic transport properties in high-mobility two-dimensional electron systems (2DES) concerns the possibility of electron hydrodynamic behavior [1–5]. This transport regime can be realized in samples of sufficient purity and only in a certain range of temperatures where the mean free path due to electron collisions ℓ_{ee} becomes short compared to other relevant length scales [6,7]. Various experiments in graphene devices, including transport measurements [8–14] and local imaging techniques [15–19], provided numerous pieces of evidence for realization of hydrodynamic electron flow.

The Corbino disk geometry [20,21] is an attractive alternative to conventional Hall effect measurements of magnetotransport properties of 2DES in rectangular devices. Thermoelectric transport in graphene Corbino devices was studied experimentally [22–27]. Hydrodynamic theory was applied to these systems to identify viscous effects in electron transport [28–33].

Because of the potential character of the flow in Corbino geometry, the manifestations of viscosity in hydrodynamic transport are rather unusual. In particular, the viscous force density vanishes. Therefore the Bernoulli law, which generally works only for ideal liquids, applies in this case [34]. Since in the creeping flow regime, which is realized in linear response, the net force density also vanishes, this means that the density of external force driving the flow vanishes as well. In the context of electron hydrodynamics, expulsion of the external force from the flow produces drops of applied voltage and temperature at the sample boundaries [31,32] which are proportional to the fluid viscosity. It is interesting to note that the energy dissipation associated with these drops occurs in the bulk of the flow. Indeed, the vanishing of the viscous force in Corbino flow does not imply vanishing of the viscous stress tensor, only its divergence. The viscous stresses

arising from the deformation of fluid elements by the flow produce the required energy dissipation.

Previous theoretical treatments of hydrodynamic magnetotransport assumed Galilean invariance of the electron liquid [30,31,35]. Therefore their results do not apply to graphene devices near charge neutrality. Motivated in part by experiments [24-27], here we develop a theory of hydrodynamic magnetotransport in graphene Corbino devices near charge neutrality. We show that the mechanism of hydrodynamic magnetoresistance (MR) in this case is qualitatively different from that in systems with Galilean-invariant electron liquid, which is caused primarily by the modification of the hydrodynamic flow by the Lorentz force [35]. The difference becomes most striking at charge neutrality, where charge current is decoupled from the hydrodynamic flow in the absence of a magnetic field. In contrast, in a nonzero field the flow remains coupled to the charge current even at charge neutrality. The mechanism of the coupling can be understood as follows. Though the electric current is caused entirely by the intrinsic conductivity, its magnitude is proportional to the electromotive force (EMF) acting on the electrons. The latter corresponds to the electric field evaluated in the frame moving with the liquid. Therefore in the presence of a magnetic field the EMF depends on the flow velocity [36]. In turn, the Lorentz force caused by the current affects the flow velocity. The magnetoresistance arising from this mechanism depends both the intrinsic conductivity and the viscosity of the electron liquid.

II. HYDRODYNAMIC DESCRIPTION

We consider a Corbino disk geometry with radii r_1 and r_2 , and aspect ratio $p = r_2/r_1 > 1$, see Fig. 1. The interior of the disk $r \in [r_1, r_2]$ is assumed to be either graphene monolayer (MLG) or bilayer (BLG); more generally, trilayer and multilayers are also possible. The device is subjected to an

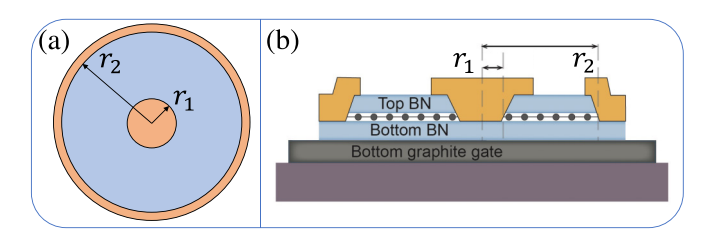


FIG. 1. Graphene Corbino disk geometry top view is depicted on panel (a). The panel (b) shows the side view of the same device, where a sheet of graphene is encapsulated between the layers of hexagonal boron nitride. The whole device is deposited on the substrate with added gate control.

external magnetic field $H = H\hat{z}$ applied perpendicular to the xy plane of the disk. We consider a setup in which a voltage V and a temperature difference ΔT are applied between the inner and outer electrodes. The electric and heat currents arising in response are denoted by, respectively, $I = eI_n$ and $I_Q = TI_s$ (for convenience we also introduce particle I_n and entropy I_s currents, where e is the electron charge and T is the temperature).

The 2×2 thermoelectric resistance matrix $\hat{\mathcal{R}}$ can be determined by equating the Joule heat \mathcal{P} to the rate of energy dissipation in the flow:

$$\mathcal{P} = \vec{\mathcal{I}}^{\mathbb{T}} \hat{\mathcal{R}} \vec{\mathcal{I}}, \quad \vec{\mathcal{I}}^{\mathbb{T}} = (I, I_0). \tag{1}$$

Here we introduced the two-component column vector of currents $\vec{\mathcal{I}}$, with the superscript \mathbb{T} denoting transposition. The linear response electrical $(R_{\rm el})$ and thermal $(R_{\rm th})$ resistances,

$$R_{\rm el}(H) = (V/I)_{\Delta T = 0}, \quad R_{\rm th}(H) = (\Delta T/I_Q)_{I=0},$$
 (2)

can be expressed in terms of the matrix elements of $\hat{\mathcal{R}}$ as follows: $R_{\rm el}(H) = {\rm Det}\hat{\mathcal{R}}/\mathcal{R}_{22}$, and $R_{\rm th}(H) = T\mathcal{R}_{22}$. The off-diagonal elements, $\mathcal{R}_{12} = \mathcal{R}_{21}$, define thermoelectric response. The Seebeck coefficient is given by $S(H) = -(V/\Delta T)_{I=0} = -\mathcal{R}_{12}/(T\mathcal{R}_{22})$. From the Onsager relation, $S = \Pi/T$, we can easily determine the Peltier coefficient $\Pi = (I_Q/I)_{\Delta T=0}$.

The dissipated power in an electron flow,

$$\mathcal{P} = \frac{1}{2} \int \Sigma_{ij} (\partial_i u_j + \partial_j u_i) d^2 r + \int \vec{\mathcal{X}}^{\mathbb{T}} \hat{\Upsilon} \vec{\mathcal{X}} d^2 r, \quad (3)$$

comprises of two independent contributions. The first term accounts for the viscous dissipation arising from the hydrodynamic transport mode. In it the stress tensor is given by [37]

$$\Sigma_{ij} = \eta(\partial_i u_i + \partial_j u_i) + (\zeta - \eta)\delta_{ij}\partial_k u_k, \tag{4}$$

where u(r) is the hydrodynamic velocity, while η and ζ are, respectively, the shear and bulk viscosities. The form of Σ_{ij} in Eq. (4) is written for two spatial dimensions. Note also that in Eq. (3) the summation over the repeated indices is implicit. The second term in Eq. (3) captures the entropy production rate due to transport in the relative mode, i.e., charge and energy transport relative to the liquid. In Eq. (3) the column vector of thermodynamic forces \tilde{X} consists of the EMF and

the temperature gradient. It can be written in the form [36]

$$\vec{\mathcal{X}} = \vec{X} - \frac{e}{c} [\mathbf{u} \times \mathbf{H}] \vec{\Xi}, \quad \vec{\Xi}^{\mathbb{T}} = (1, 0).$$
 (5)

The first piece in the expression above is given by a pure gradient, $\vec{X} = (-eE, \nabla T)$, where eE represents the potential part of the EMF defined by the gradient of electrochemical potential. The second term above describes the contribution to EMF arising from the motion of the liquid in the presence of a magnetic field. The sum of the two contributions corresponds to evaluating the electric field in the frame moving with the liquid [36]. Finally, the matrix $\hat{\Upsilon}$ in Eq. (3) characterizes the dissipative properties of the electron liquid. In the absence of Galilean invariance, it is given by

$$\hat{\Upsilon} = \begin{pmatrix} \sigma/e^2 & \gamma/T \\ \gamma/T & \kappa/T \end{pmatrix} \tag{6}$$

and consists of the thermal conductivity κ , the intrinsic conductivity σ , and the thermoelectric coefficient γ , see Refs. [38,39]. For Galilean-invariant liquids, we have $\sigma = \gamma = 0$. In the consideration below we neglect the dependence of the kinetic coefficients in Eq. (6) on the magnetic field. This approximation assumes that ℓ_{ee} is shorter than the electron cyclotron radius. We will see that the effects considered below lead to magnetoresistance that becomes strong at very weak magnetic fields, where this approximation is justified.

In order to determine \mathcal{P} in Eq. (3) as a quadratic form of the currents I and I_Q , we need to determine the flow pattern, i.e., the spatial profile of u(r) and $\vec{X}(r)$. The hydrodynamic velocity is related to the driving forces by the Navier-Stokes (NS) equation,

$$\eta \nabla^2 \boldsymbol{u} + \zeta \nabla (\nabla \cdot \boldsymbol{u}) = \vec{x}^{\mathrm{T}} \vec{X} + [\boldsymbol{j}_n \times \hat{\boldsymbol{z}}]/l_H^2, \tag{7}$$

which expresses the force balance condition in the bulk of the flow. The first term on the right-hand side of Eq. (7) describes the potential force on the liquid, which is caused by the temperature and voltage bias. In it we introduced a two-component column vector $\vec{x}^T = (n, s)$, whose components are the densities of particles n and entropy s. The last term on the right-hand side of Eq. (7) is the Lorentz force, where j_n is the particle current density, and we introduced the magnetic length $l_H = \sqrt{c/|e|H}$.

The remaining hydrodynamic equations are given by the continuity equations for the particle current j_n and entropy current j_s . Using the column vector notation $\vec{J}^T = (j_n, j_s)$ they can be written as

$$\nabla \cdot \vec{J} = 0, \quad \vec{J} = \vec{x}u - \hat{\Upsilon}\vec{\mathcal{X}}. \tag{8}$$

In the absence of a magnetic field the flow is purely radial. The corresponding thermoelectric matrix, and the distribution of temperature and the electric potential, were determined in our previous work [32]. In the present study we extend this analysis to study thermoelectric transport in weak magnetic fields.

III. MAGNETOFLOW PATTERN

The magnetohydrodynamic description of electron liquids formulated above applies to any device geometry and does not assume Galilean invariance of the electron liquid. To make further progress, we specialize to the Corbino geometry and work in polar coordinates (r, ϕ) . Owing to the angular symmetry of the Corbino disk, the radial and azimuthal components of the currents and forces do not depend on the polar angle ϕ . Therefore, the NS equation (7) projected onto the radial (r) and azimuthal (ϕ) directions reduces to two coupled equations:

$$(\eta + \zeta)\hat{\Delta}u_r - \vec{x}^{\mathrm{T}}\vec{X}_r - (j_n)_{\phi}/l_H^2 = 0, \tag{9a}$$

$$\eta \hat{\Delta} u_{\phi} + (j_n)_r / l_H^2 = 0.$$
(9b)

Here $\hat{\Delta}$ denotes the radial component of the Laplace operator, $\hat{\Delta} = \frac{1}{r} \frac{d}{dr} (r \frac{d}{dr}) - \frac{1}{r^2}$, and the azimuthal component of the particle current density is given by

$$(j_n)_{\phi} = nu_{\phi} + \frac{\sigma}{e^2} \frac{u_r}{l_H^2}.$$
 (10)

The continuity equation (8) for the current densities reads

$$\vec{J}_r = \frac{\vec{I}}{2\pi r} = \vec{x}u_r - \hat{\Upsilon}\vec{X}_r - \hat{\Upsilon}\vec{\Xi}\frac{u_\phi}{l_H^2},\tag{11}$$

where $\vec{I}^{T} = (I_n, I_s)$ is the column vector of particle and entropy currents. In these notations the NS equation for the angular component of the hydrodynamic velocity [Eq. (9b)] reduces to the equation

$$\hat{\Delta}u_{\phi} = -\frac{I_n}{2\pi r \eta l_H^2}.$$
 (12)

Its solution is given by

$$u_{\phi}(r) = -\frac{I_n r_1}{4\pi \eta l_H^2} \left(A\rho + \frac{B}{\rho} + \rho \ln \rho \right), \tag{13}$$

where we introduced a dimensionless radial coordinate $\rho = r/r_1 \in [1, p]$. The values of the integration constants A and B are determined by the boundary conditions. Assuming the standard no-slip boundary condition $u_{\phi}(r_{1,2}) = 0$ we obtain $A = -B = -p^2 \ln p/(p^2 - 1)$.

Next, we analyze the radial part of the NS equation (9a). For this purpose we use the continuity equation (11) to express \vec{X}_r in terms of $u_{r,\phi}$. Then, using Eq. (10) we obtain

$$(k_H^2 - \hat{\Delta})u_r = \frac{\vec{x}^{\mathbb{T}} \hat{\Upsilon}^{-1} \vec{l}}{2\pi r(\eta + \zeta)}, \quad k_H^2 = \frac{1}{l^2} + \frac{\sigma}{e^2(\eta + \zeta)l_H^4},$$
(14)

where the characteristic length scale l is given by

$$l^{-2} = \frac{\vec{x}^{\mathrm{T}} \hat{\Upsilon}^{-1} \vec{x}}{(\eta + \zeta)} = \frac{\frac{n^2 \kappa}{T} - \frac{2ns\gamma}{T} + \frac{s^2 \sigma}{e^2}}{(\eta + \zeta) \left(\frac{\kappa \sigma}{Tc^2} - \frac{\gamma^2}{T^2}\right)}.$$
 (15)

We note that in graphene the bulk viscosity is expected to be negligible [40,41]. Therefore, it will be omitted in what follows.

To motivate further approximations it is useful to estimate the order of magnitude of l in different transport regimes. For instance, in the case of MLG in the low-density limit close to charge neutrality (Dirac fluid), one gets $l \approx \sqrt{\kappa \eta/T s^2} \sim l_T$, where $l_T = v/T$ is the thermal de Broglie length. To arrive at this estimation we have used s, $\eta \propto (T/v)^2$ and $\kappa \propto T$ near

the neutrality point [42]. In the high-density regime (Fermi liquid), one has instead $l \approx \sqrt{\eta/n^2} \sim l_T$, where we have used the estimation of viscosity $\eta \sim n(E_F/T)^2$ in the Fermi liquid regime [43]. The field dependence of k_H , and thus u_r , is manifested through the parameter $l^2/(\eta l_H^4) \sim (l_T/l_H)^4 \ll 1$, which is negligible in the hydrodynamic regime since l_T is a microscopic length scale. Consequently, we can set $k_H^2 = l^{-2}$, thereby neglecting the dependence of u_r on the magnetic field. This is accurate within our approximation, in which we neglect the field dependence of the viscosities η and ζ , and the kinetic coefficients in matrix $\hat{\Upsilon}$.

The solution of Eq. (14) consists of the general solution of the homogeneous equation and the particular solution of the inhomogeneous equation. In our approximation the former is given by a linear combination of modified Bessel functions of the first and second kinds, $I_1(r/l)$ and $K_1(r/l)$. These exponentially decaying and growing solutions of a homogeneous equation are localized on the length l near the inner and outer boundaries and describe deviations of the hydrodynamic flow from that in the bulk. These solutions contribute to the thermoelectric resistance of the contacts. We are interested in the contribution to the resistance matrix due to the hydrodynamic flow in the interior of the disk. The latter corresponds to the particular solution, which is given by

$$u_r(r) = \frac{1}{2\pi r} \frac{\vec{x}^{\mathbb{T}} \hat{\Upsilon}^{-1} \vec{I}}{\vec{x}^{\mathbb{T}} \hat{\Upsilon}^{-1} \vec{x}}.$$
 (16)

Note that for given charge and heat currents the radial component of the flow is independent of the magnetic field. In contrast, the azimuthal component of the flow velocity in Eq. (13) does get modified by the magnetic field. The strength of this modification is characterized by a single dimensionless parameter $\beta = nr_1^2/(2\eta l_H^4)$. This parameter measures the relative strength of the Lorentz and viscous Stokes forces and determines the number of turns the flow makes between the electrodes. For $\beta > 1$ the flow swirls around electrodes the integer of β times.

To illustrate the hydrodynamic magnetoflow in Fig. 2, we took $\beta=0.5$ and used Eqs. (13) and (16) for a particular biasing scenario with $I_s \to 0$ at the high-density limit $n\gg s$. The velocity in the resulting flow pattern is normalized to $u_0=I_n/(2\pi r_1 n)$. It is worth noting that in the situation corresponding to charge neutrality, $n\to 0$, the radial component of the flow velocity in Eq. (16) vanishes and the charge transport occurs only through the relative mode. In contrast, the azimuthal component u_ϕ remains nonzero in the presence of a magnetic field, so that hydrodynamic magnetoflow at charge neutrality is purely vortical.

IV. VISCOUS MAGNETORESISTANCE

Let us now determine the rate of energy dissipation in this hydrodynamic transport. The derivation naturally breaks down into two steps. First, we use $u_r(r)$ and $u_{\phi}(r)$ to determine the nonvanishing components of the stress tensor:

$$\Sigma_{rr} = 2\eta \frac{\partial u_r}{\partial r}, \quad \Sigma_{\phi\phi} = 2\eta \frac{u_r}{r}, \quad \Sigma_{r\phi} = \eta \left(\frac{\partial u_\phi}{\partial r} - \frac{u_\phi}{r} \right).$$
 (17)

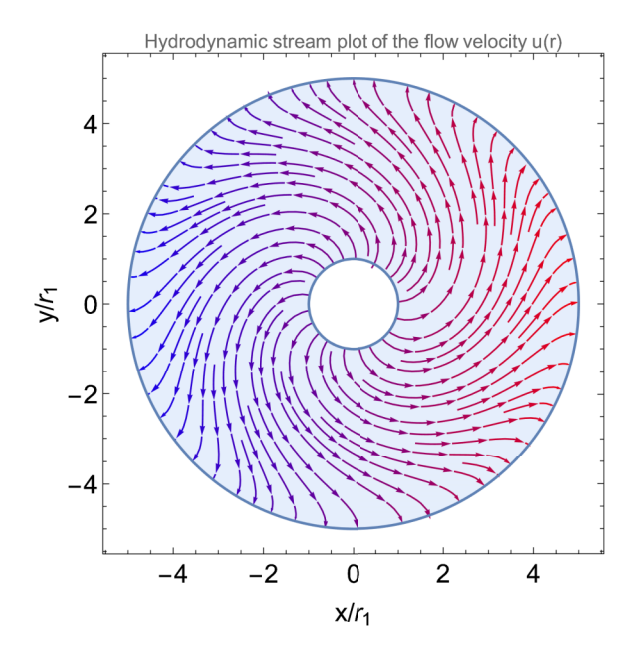


FIG. 2. Illustration of hydrodynamic flow of electron liquid in a Corbino device in a perpendicular magnetic field. The stream plot for the velocity u(r) is generated for the disk with the inner to outer radius ratio $p = r_2/r_1 = 5$ and non-slip boundary conditions.

These expressions enable us to calculate the first term in Eq. (3). The second step is to resolve the continuity equation (11) in order to determine the radial dependence of the forces in the bulk of the flow $\vec{X}_r(r)$. The particular expressions we need read

$$eE_r = \frac{1}{\text{Det}\hat{\Upsilon}} \left[\left(\frac{s\gamma}{T} - \frac{n\kappa}{T} \right) u_r + \frac{\kappa}{T} \frac{I_n}{2\pi r} - \frac{\gamma}{T} \frac{I_s}{2\pi r} \right] + \frac{u_\phi}{l_H^2},$$
(18a)

$$\nabla_r T = \left[\left(\frac{s\sigma}{e^2} - \frac{n\gamma}{T} \right) u_r + \frac{\gamma}{T} \frac{I_n}{2\pi r} - \frac{\sigma}{e^2} \frac{I_s}{2\pi r} \right]. \tag{18b}$$

These terms define the second contribution to \mathcal{P} in Eq. (3), which stems from the relative mode. The remaining spatial integrations are elementary but yield cumbersome expressions. Below we focus on the regime near charge neutrality working in leading order in $n/s \ll 1$, and furthermore retain only the leading correction in the magnetic field dependence.

For the electrical and thermal magnetoresistance we thus find

$$R_{\rm el}(H) = R_0 \left[1 + \frac{\sigma}{e^2} \frac{r_2^2}{\eta l_H^4} f_1(p) \right], \ R_0 = \frac{\ln p}{2\pi \sigma},$$
 (19a)

$$R_{\text{th}}(H) = R_{\text{th}} \left[1 + \frac{\sigma}{e^2} \frac{r_2^2}{\eta l_H^4} f_2(p) \right], \ R_{\text{th}} = \frac{\eta(p^2 - 1)}{\pi T (r_2 s)^2}, \ (19b)$$

where the dimensionless functions of the aspect ratio are $f_1(p) = \frac{(p^2-1)^2-4p^2\ln^2p}{8p^2(p^2-1)\ln p}$, and $f_2(p) = \frac{\ln p}{2(p^2-1)}$. In order to extract the thermopower we must retain finite density. In the limit $n/s \ll 1$ we determine

$$S(H) = S_0 \left[1 - \frac{\sigma}{e^2} \frac{r_2^2}{\eta l_H^4} f_2(p) \right], \ S_0 = \frac{1}{e} \frac{ns}{n^2 + \Gamma^2}.$$
 (20)

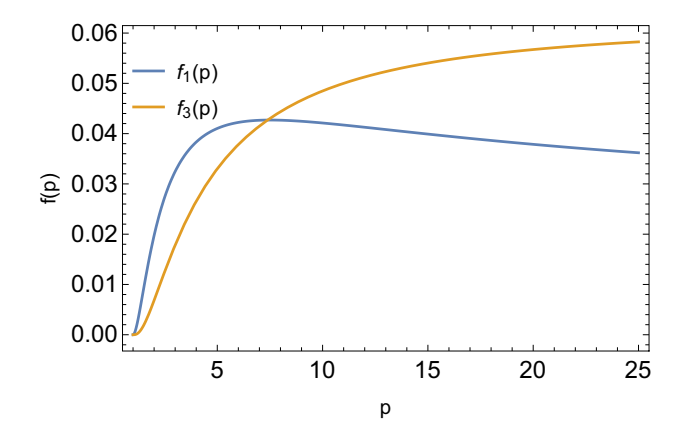


FIG. 3. Dependence of the dimensionless functions $f_{1,3}(p)$ that define MR in Eqs. (19) and (21) on the aspect ratio of the Corbino disk.

The characteristic width in the density dependence across the charge neutrality is given by $\Gamma^2 = \frac{\sigma}{e^2} \frac{2\eta(p^2-1)}{r_2^2 \ln p}$. It corresponds to electron densities, which are much smaller than the characteristic thermal density s.

We see that, just as for Galilean-invariant liquids [35], MR is positive, but its magnitude is proportional to the intrinsic conductivity and inversely proportional to the viscosity of the electron liquid. The temperature dependence of MR is primarily governed by the fluid viscosity since the intrinsic conductivity is only weakly T dependent. From the weak-coupling analysis, it is known that σ behaves logarithmically with temperature [44–46]. The inverse proportionality of MR to the viscosity is consistent with the earlier results for correlated electron liquids subject to long-range disorder potential [35,47]. This behavior seems to be universal in the hydrodynamic regime. Indeed, extending the above analysis to the opposite limit of high density, $n \gg s$, one finds for MR

$$R_{\rm el}(H) = R_0 + \frac{1}{\pi e^2} \frac{r_2^2}{\eta l_H^4} f_3(p), \ R_0 = \frac{\eta(p^2 - 1)}{\pi e^2 (r_2 n)^2},$$
 (21)

with $f_3(p) = \frac{p^2-1}{16p^2} \left[1 - \frac{4p^2 \ln^2 p}{(p^2-1)^2}\right]$. We note that the functions $f_1(p)$ and $f_3(p)$, which characterize the magnitude of MR in Eqs. (19) and (21), exhibit sensitive dependence on the aspect ratio p. As illustrated in Fig. 3, these functions range between zero at $p \to 1$ and practically saturate for p > 10.

It is worth noting that at charge neutrality magnetoresistance in Eq. (19) reaches a value of order unity at rather small fields, where $l_H^2 \sim r_1 l_T$, and our approximation of neglecting the dependence of the kinetic coefficients in Eq. (6) and k_H in Eq. (14) on the magnetic field still holds. At large densities MR becomes independent of the intrinsic conductivity. In this regime the absence of Galilean invariance becomes inessential.

V. CONCLUSION

In conclusion, to facilitate possible comparison to experiments, we present estimates for relative MR for both electrical and thermal parts. It is convenient to express them in the

form $\delta R_{\rm el,th}(H) = A_{\rm el,th}H^2$, where the factors $A_{\rm el,th}(n,T)$ can be measured independently. Exactly at charge neutrality, we determine that their ratio is $A_{\rm el}/A_{\rm th} \propto T s^2/\eta$. For MLG devices, we thus expect $A_{\rm el}/A_{\rm th} \propto T^3$. In BLG, $\eta(T)$ has not been microscopically calculated near charge neutrality, since this is a problem of strong-coupling theory. Nevertheless, we can infer the temperature dependence of η from the viscosity to entropy density bound conjecture [48]. It thus suggests $\eta \sim s(T) \sim m^*T$, where m^* is the effective mass of the band structure. Therefore, for BLG we expect $A_{\rm el}/A_{\rm th} \propto T^2$.

Note added. Recently we became aware of the related work of Ref. [49] that also addresses MR in a graphene Corbino disk at charge neutrality.

- [1] B. Spivak, S. V. Kravchenko, S. A. Kivelson, and X. P. A. Gao, Colloquium: Transport in strongly correlated two dimensional electron fluids, Rev. Mod. Phys. 82, 1743 (2010).
- [2] B. N. Narozhny, I. V. Gornyi, A. D. Mirlin, and J. Schmalian, Hydrodynamic approach to electronic transport in graphene, Ann. Phys. 529, 1700043 (2017).
- [3] A. Lucas and K. C. Fong, Hydrodynamics of electrons in graphene, J. Phys.: Condens. Matter **30**, 053001 (2018).
- [4] A. Levchenko and J. Schmalian, Transport properties of strongly coupled electron–phonon liquids, Ann. Phys. 419, 168218 (2020).
- [5] M. Polini and A. K. Geim, Viscous electron fluids, Phys. Today 73, 28 (2020).
- [6] R. N. Gurzhi, Hydrodynamic effects in solids at low temperature, Sov. Phys. Usp. 11, 255 (1968).
- [7] A. V. Andreev, S. A. Kivelson, and B. Spivak, Hydrodynamic Description of Transport in Strongly Correlated Electron Systems, Phys. Rev. Lett. 106, 256804 (2011).
- [8] J. Crossno, J. K. Shi, K. Wang, X. Liu, A. Harzheim, A. Lucas, S. Sachdev, P. Kim, T. Taniguchi, K. Watanabe, T. A. Ohki, and K. C. Fong, Observation of the Dirac fluid and the breakdown of the Wiedemann-Franz law in graphene, Science 351, 1058 (2016).
- [9] F. Ghahari, H.-Y. Xie, T. Taniguchi, K. Watanabe, M. S. Foster, and P. Kim, Enhanced Thermoelectric Power in Graphene: Violation of the Mott Relation by Inelastic Scattering, Phys. Rev. Lett. 116, 136802 (2016).
- [10] D. A. Bandurin, I. Torre, R. K. Kumar, M. B. Shalom, A. Tomadin, A. Principi, G. H. Auton, E. Khestanova, K. S. Novoselov, I. V. Grigorieva, L. A. Ponomarenko, A. K. Geim, and M. Polini, Negative local resistance caused by viscous electron backflow in graphene, Science 351, 1055 (2016).
- [11] R. Krishna Kumar, D. A. Bandurin, F. M. D. Pellegrino, Y. Cao, A. Principi, H. Guo, G. H. Auton, M. Ben Shalom, L. A. Ponomarenko, G. Falkovich, K. Watanabe, T. Taniguchi, I. V. Grigorieva, L. S. Levitov, M. Polini, and A. K. Geim, Superballistic flow of viscous electron fluid through graphene constrictions, Nat. Phys. 13, 1182 (2017).
- [12] Y. Nam, D.-K. Ki, D. Soler-Delgado, and A. F. Morpurgo, Electron–hole collision limited transport in charge-neutral bilayer graphene, Nat. Phys. 13, 1207 (2017).
- [13] D. A. Bandurin, A. V. Shytov, L. S. Levitov, R. K. Kumar, A. I. Berdyugin, M. Ben Shalom, I. V. Grigorieva, A. K. Geim,

ACKNOWLEDGMENTS

We thank V. Gall, I. Gornyi, S. Ilani, P. Kim, B. Narozhny, A. Talanov, and J. Waissman for insightful discussions. This work at the UW-Madison was financially supported by the National Science Foundation through Grants No. DMR-2203411 (A.L.) and DMR-1653661 (S.L.). The work of A.V.A. was supported, in part, by the US National Science Foundation through the MRSEC Grant No. DMR-1719797, the Thouless Institute for Quantum Matter, and the College of Arts and Sciences at the University of Washington. A.L. is grateful to the Abdus Salam ICTP for hospitality, where this work was finalized during the meeting titled "Strongly Correlated Matter: From Quantum Criticality to Flat Bands."

- and G. Falkovich, Fluidity onset in graphene, Nat. Commun. 9, 4533 (2018).
- [14] A. I. Berdyugin, S. G. Xu, F. M. D. Pellegrino, R. K. Kumar, A. Principi, I. Torre, M. B. Shalom, T. Taniguchi, K. Watanabe, I. V. Grigorieva, M. Polini, A. K. Geim, and D. A. Bandurin, Measuring Hall viscosity of graphene electron fluid, Science 364, 162 (2019).
- [15] J. A. Sulpizio, L. Ella, A. Rozen, J. Birkbeck, D. J. Perello, D. Dutta, M. Ben-Shalom, T. Taniguchi, K. Watanabe, T. Holder, R. Queiroz, A. Principi, A. Stern, T. Scaffidi, A. K. Geim, and S. Ilani, Visualizing Poiseuille flow of hydrodynamic electrons, Nature (London) 576, 75 (2019).
- [16] M. J. H. Ku, T. X. Zhou, Q. Li, Y. J. Shin, J. K. Shi, C. Burch, L. E. Anderson, A. T. Pierce, Y. Xie, A. Hamo, U. Vool, H. Zhang, F. Casola, T. Taniguchi, K. Watanabe, M. M. Fogler, P. Kim, A. Yacoby, and R. L. Walsworth, Imaging viscous flow of the Dirac fluid in graphene, Nature (London) 583, 537 (2020).
- [17] Z. J. Krebs, W. A. Behn, S. Li, K. J. Smith, K. Watanabe, T. Taniguchi, A. Levchenko, and V. W. Brar, Imaging the breaking of electrostatic dams in graphene for ballistic and viscous fluids, arXiv:2106.07212.
- [18] C. Kumar, J. Birkbeck, J. A. Sulpizio, D. J. Perello, T. Taniguchi, K. Watanabe, O. Reuven, T. Scaffidi, A. Stern, A. K. Geim, and S. Ilani, Imaging hydrodynamic electrons flowing without Landauer-Sharvin resistance, Nature (London) 609, 276 (2022).
- [19] A. Jenkins, S. Baumann, H. Zhou, S. A. Meynell, Y. Daipeng, K. Watanabe, T. Taniguchi, A. Lucas, A. F. Young, and A. C. Bleszynski Jayich, Imaging the Breakdown of Ohmic Transport in Graphene, Phys. Rev. Lett. 129, 087701 (2022).
- [20] O. M. Corbino, Azioni elettromagnetiche doyute agli ioni dei metalli deviati dalla traiettoria normale per effetto di un campo, Nuovo Cim 1, 397 (1911).
- [21] G. P. Carver, A Corbino disk apparatus to measure Hall mobilities in amorphous semiconductors, Rev. Sci. Instrum. 43, 1257 (1972).
- [22] J. Yan and M. S. Fuhrer, Charge transport in dual gated bilayer graphene with Corbino geometry, Nano Lett. 10, 4521 (2010).
- [23] C. Faugeras, B. Faugeras, M. Orlita, M. Potemski, R. R. Nair, and A. K. Geim, Thermal conductivity of graphene in Corbino membrane geometry, ACS Nano 4, 1889 (2010).
- [24] Y. Zhao, P. Cadden-Zimansky, F. Ghahari, and P. Kim, Magnetoresistance Measurements of Graphene at the Charge Neutrality Point, Phys. Rev. Lett. 108, 106804 (2012).

- [25] Y. Zeng, J. I. A. Li, S. A. Dietrich, O. M. Ghosh, K. Watanabe, T. Taniguchi, J. Hone, and C. R. Dean, High-Quality Magnetotransport in Graphene Using the Edge-Free Corbino Geometry, Phys. Rev. Lett. 122, 137701 (2019).
- [26] M. Real, D. Gresta, C. Reichl, J. Weis, A. Tonina, P. Giudici, L. Arrachea, W. Wegscheider, and W. Dietsche, Thermoelectricity in Quantum Hall Corbino Structures, Phys. Rev. Appl. 14, 034019 (2020).
- [27] M. Kamada, V. Gall, J. Sarkar, M. Kumar, A. Laitinen, I. Gornyi, and P. Hakonen, Strong magnetoresistance in a graphene Corbino disk at low magnetic fields, Phys. Rev. B 104, 115432 (2021).
- [28] A. Tomadin, G. Vignale, and M. Polini, Corbino Disk Viscometer for 2D Quantum Electron Liquids, Phys. Rev. Lett. 113, 235901 (2014).
- [29] B. N. Narozhny, I. V. Gornyi, M. Titov, M. Schütt, and A. D. Mirlin, Hydrodynamics in graphene: Linear-response transport, Phys. Rev. B 91, 035414 (2015).
- [30] T. Holder, R. Queiroz, and A. Stern, Unified Description of the Classical Hall Viscosity, Phys. Rev. Lett. 123, 106801 (2019).
- [31] M. Shavit, A. Shytov, and G. Falkovich, Freely Flowing Currents and Electric Field Expulsion in Viscous Electronics, Phys. Rev. Lett. 123, 026801 (2019).
- [32] S. Li, A. Levchenko, and A. V. Andreev, Hydrodynamic thermoelectric transport in Corbino geometry, Phys. Rev. B 105, 125302 (2022).
- [33] V. Gall, B. N. Narozhny, and I. V. Gornyi, Electronic viscosity and energy relaxation in neutral graphene, arXiv:2206.07414.
- [34] T. E. Faber, Fluid Dynamics for Physicists, 1st ed. (Cambridge University Press, Cambridge, England, 1995).
- [35] A. Levchenko, H.-Y. Xie, and A. V. Andreev, Viscous magnetoresistance of correlated electron liquids, Phys. Rev. B 95, 121301(R) (2017).
- [36] L. D. Landau and E. M. Lifshitz, *Electrodynamics of Continuous Media*, 2nd ed., Course of Theoretical Physics, Vol. 8 (Butterworth-Heinemann, Oxford, 1984).

- [37] L. D. Landau and E. M. Lifshitz, *Fluid Mechanics*, 2nd ed., Course of Theoretical Physics, Vol. 6 (Butterworth-Heinemann, Oxford, 1987).
- [38] M. Müller and S. Sachdev, Collective cyclotron motion of the relativistic plasma in graphene, Phys. Rev. B 78, 115419 (2008).
- [39] M. S. Foster and I. L. Aleiner, Slow imbalance relaxation and thermoelectric transport in graphene, Phys. Rev. B 79, 085415 (2009).
- [40] A. Principi, G. Vignale, M. Carrega, and M. Polini, Bulk and shear viscosities of the two-dimensional electron liquid in a doped graphene sheet, Phys. Rev. B 93, 125410 (2016).
- [41] B. N. Narozhny, Electronic hydrodynamics in graphene, Ann. Phys. 411, 167979 (2019).
- [42] M. Müller, J. Schmalian, and L. Fritz, Graphene: A Nearly Perfect Fluid, Phys. Rev. Lett. 103, 025301 (2009).
- [43] A. A. Abrikosov and I. M. Khalatnikov, The theory of a Fermi liquid (the properties of liquid 3He at low temperatures), Rep. Prog. Phys. **22**, 329 (1959).
- [44] E. G. Mishchenko, Effect of Electron-Electron Interactions on the Conductivity of Clean Graphene, Phys. Rev. Lett. 98, 216801 (2007).
- [45] L. Fritz, J. Schmalian, M. Müller, and S. Sachdev, Quantum critical transport in clean graphene, Phys. Rev. B 78, 085416 (2008).
- [46] A. B. Kashuba, Conductivity of defectless graphene, Phys. Rev. B 78, 085415 (2008).
- [47] A. A. Patel, R. A. Davison, and A. Levchenko, Hydrodynamic flows of non-Fermi liquids: Magnetotransport and bilayer drag, Phys. Rev. B 96, 205417 (2017).
- [48] P. K. Kovtun, D. T. Son, and A. O. Starinets, Viscosity in Strongly Interacting Quantum Field Theories from Black Hole Physics, Phys. Rev. Lett. 94, 111601 (2005).
- [49] V. Gall, B. N. Narozhny, and I. V. Gornyi (unpublished).